

*The Cryosphere*

Supporting Information for

## **Larger variability of winter snow depth promotes the soil thermal regime instability over boreal high latitudes**

**Lingyun Ai<sup>1</sup>, Kai Yang<sup>2\*</sup>, Feimin Zhang<sup>1</sup>, Chenghai Wang<sup>1</sup>, Tonghua Wu<sup>3</sup>, Qi Qi<sup>1</sup>, Haohui Li<sup>1</sup>**

<sup>1</sup>Key Laboratory of Climate Resource Development and Disaster Prevention of Gansu Province, Research and Development Center of Earth System Model, College of Atmospheric Sciences, Lanzhou University, Lanzhou 730000, China.

<sup>2</sup>Institute of Mountain Hazards and Environment, Chinese Academy of Sciences, Chengdu, 610299, China

<sup>3</sup>Cryosphere Research Station on the Qinghai-Tibet Plateau, State Key Laboratory of Cryospheric Science and Frozen Soil Engineering, Northwest Institute of Eco-Environment and Resource, Chinese Academy of Sciences, Lanzhou, 730000, China

\*Corresponding author: K. Yang, [kaiyang@imde.ac.cn](mailto:kaiyang@imde.ac.cn)

### **Contents of this file**

Supplementary Note 1

Tables S1

Figures S1 to S4

## Supplementary Note 1 Merged soil temperature dataset

Seven reanalysis datasets (ERA5, ERA5-Land, GLDAS-Noah, FLDAS, CFSR, CFSv2, MERRA2; Table S1) were used to create a merged monthly soil temperature dataset at depths of 40 cm and 160 cm. All datasets were converted to the  $0.5^\circ \times 0.625^\circ$  (latitude  $\times$  longitude) spatial resolution. The 40 cm soil temperature data from ERA5 and ERA5-Land are generated using the upper three soil layers (0–7 cm, 7–28 cm, and 28–100 cm), while the 160 cm soil temperature is represented by data from the 100–89 cm layer. For GLDAS-Noah, CFSR, CFSv2, and FLDAS, the 40 cm soil temperature is derived from the upper three layers (0–10 cm, 10–40 cm, and 40–100 cm), and the 160 cm soil temperature corresponds to the 100–200 cm layer. For MERRA2, the 40 cm soil temperature is represented by the third layer (29.4–67.99 cm), and the 160 cm soil temperature is calculated using layers 67.99–144.25 cm and 144.25–294.96 cm.

The merged soil temperature dataset was constructed by selecting optimal combinations with the highest skill score in describing both soil temperature magnitude and its standard deviation. Unfortunately, most of the available reanalysis datasets (i.e., GLDAS-Noah, CFSR, CFSv2, FLDAS) only provide soil temperature data at layer 0–200 cm, thus, the depths of the merged soil temperature dataset was limited to the 40 and 160 cm. For soil temperature at the 40 cm depth over the continuous permafrost region, the merged dataset was constructed by combining ERA5, GLDAS, and MERRA2. For soil temperature at the 160 cm depth, ERA5 and MERRA2 were selected and a simple ensemble average of seven reanalysis datasets was used for the remaining land areas. Finally, the monthly merged soil temperature dataset was produced at depths of 40 cm and 160 cm, covering the period from 1982 to 2022 with a  $0.5^\circ \times 0.625^\circ$  (latitude  $\times$  longitude) spatial resolution.

The near-surface (2-meter) air temperature and wind data was obtained from the fifth-generation ECMWF atmospheric reanalysis (ERA5) which evolved from ERA-Interim. It had a spatial resolution of  $0.25^\circ \times 0.25^\circ$  from 1981 to 2018.

The observations at 40 cm and 160 cm depths were used to evaluate the reliability of the merged soil temperature dataset, by using the Taylor skill score ( $T$ ), mean bias error ( $MBE$ ) and Root Mean Square Error ( $RMSE$ ), and it outperformed all individual reanalysis products (Figure S1).

The formulas for  $T$ ,  $MBE$  and  $RMSE$  are as follows:

$$T = \frac{2(1+R)}{(\sigma+1/\sigma)^2} \quad (S1)$$

$$MBE = \frac{1}{n} \sum_{i=1}^n (X_{G,i} - X_{O,i}) \quad (S2)$$

$$RMSE = \sqrt{\frac{\sum_{i=1}^n (X_{G,i} - X_{O,i})^2}{n}} \quad (S3)$$

where  $R$  is the correlation between observation and each reanalysis dataset, and  $\sigma$  is the ratio of standard deviation of reanalysis dataset to that of observation.  $X_{G,i}$  and  $X_{O,i}$  represent the simulated value and observed value, respectively,  $n$  represents the sequence length.

**Table S1.** Detailed information of reanalysis datasets used for the monthly merged soil temperature dataset.

| Resolution    | Product    | Data period  | Land model    | Depth (cm)   |
|---------------|------------|--------------|---------------|--|
| 0.1 °×0.1 °   | ERA5-Land  | 1950–present | HTESSEL       | 0–7, 7–28, 28–100, 100–289                                 |
| 0.25 °×0.25 ° | ERA5       | 1940–present | HTESSEL       | 0–7, 7–28, 28–100, 100–289                                 |
| 0.25 °×0.25 ° | GLDAS-Noah | 1948–present | Noah LSM      | 0–10, 10–40, 40–100, 100–200                               |
| 0.5 °×0.5 °   | CFSR       | 1979–2010    | Noah LSM      | 0–10, 10–40, 40–100, 100–200                               |
| 0.5 °×0.5 °   | CFSv2      | 2011–present | Noah LSM      | 0–10, 10–40, 40–100, 100–200                               |
| 0.1 °×0.1 °   | FLDAS      | 1982–present | Noah LSM      | 0–10, 10–40, 40–100, 100–200                               |
| 0.5 °×0.625 ° | MERRA2     | 1980–present | Catchment LSM | 0–9.88, 9.88–29.4, 29.4–67.99, 67.99–144.25, 144.25–294.96 |

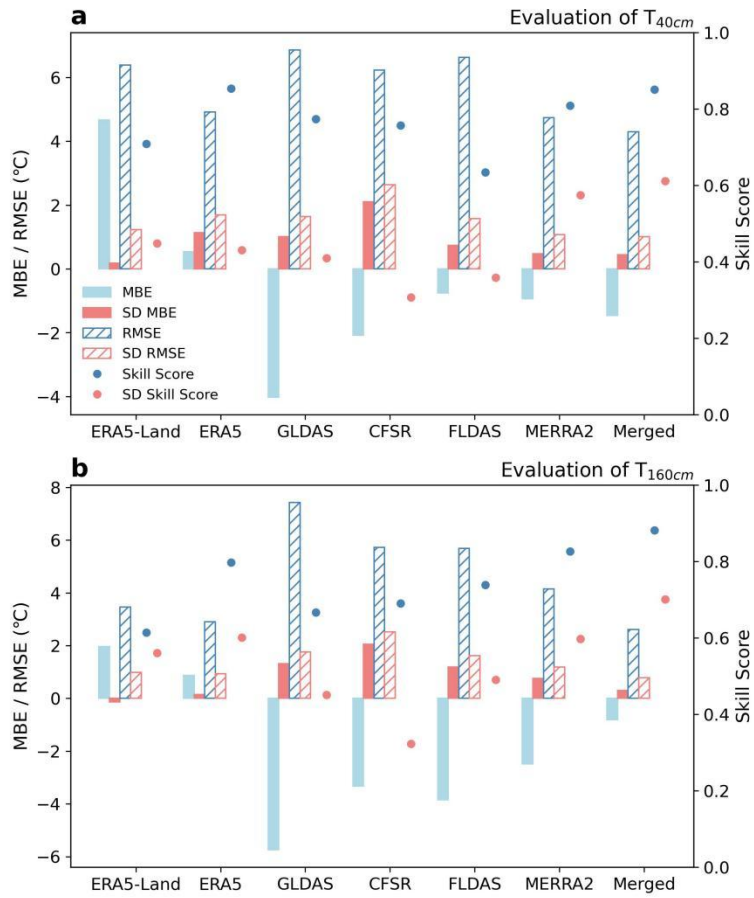


**Figure S1.** Evaluations of the merged soil temperature ( $T_{\text{soil}}$ ) dataset. Skill score, MEB and RMSE (Supplementary Note 1) for winter (December–January–February) soil temperature (1982–2022) and soil temperature standard deviation (SD; 1986–2018) at (a) 40 cm depth and (b) 160 cm depth.

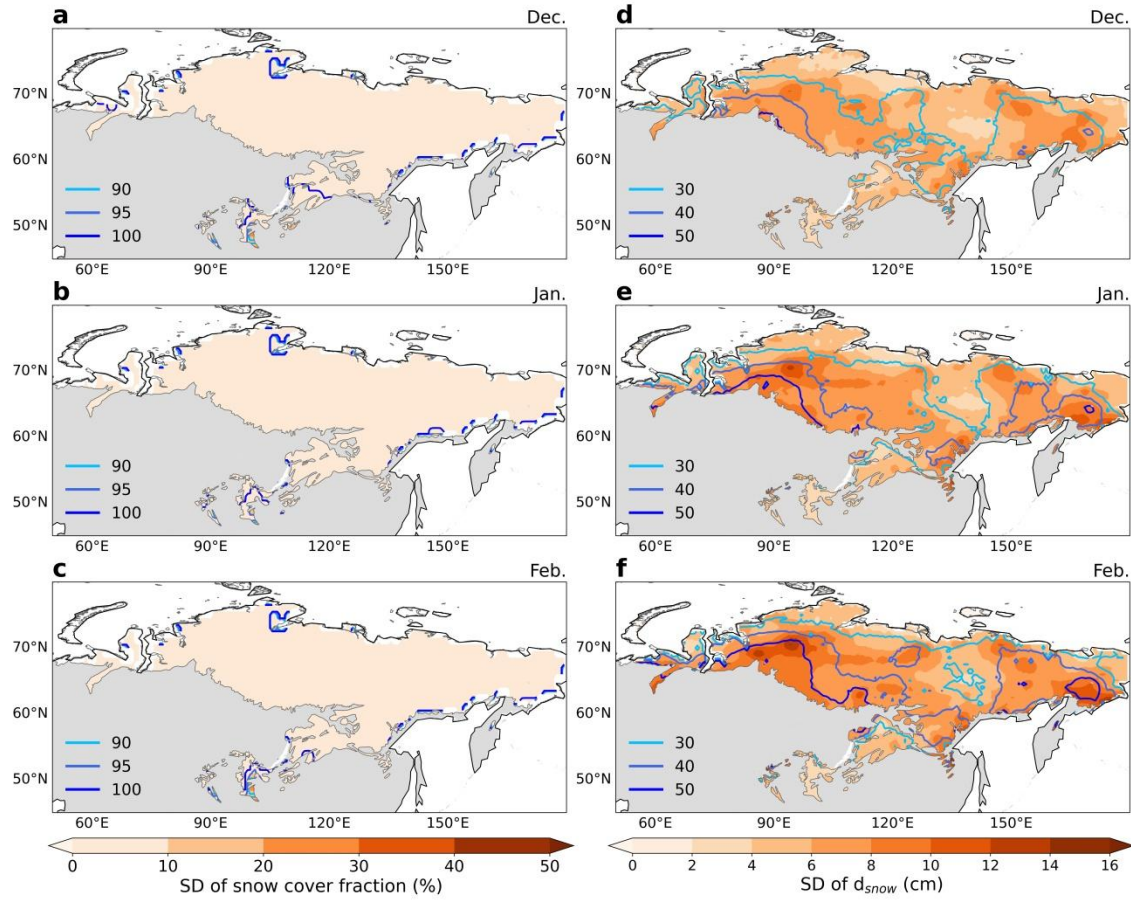


**Figure S2.** Interannual variability of snow cover fraction and snow thickness in winter (December–January–February). Spatial distribution of SD (shading) and multi-year (1993–2013) average (contour lines) of (a–c) snow cover fraction (%), (d–f) snow depth ( $d_{\text{snow}}$ ) in winter. Snow cover fraction data was provided by the National Snow and Ice Data Center (NSIDC), version 4, with a spatial resolution of 25 kilometers using the Equal Area Scalable Earth (EASE) grid 2.0 projection. Monthly snow cover fraction data is derived by averaging the weekly data and then converted to a regular grid with a spatial resolution of  $1^{\circ} \times 1^{\circ}$ .

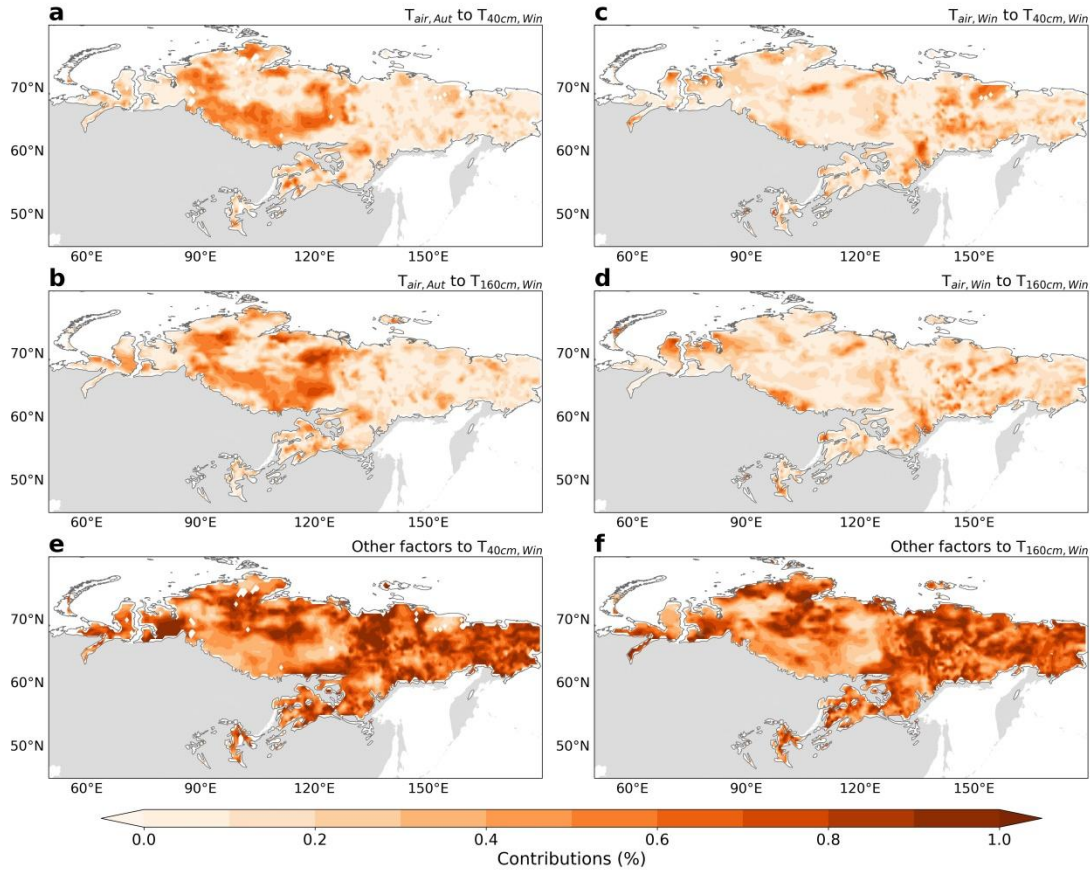


**Figure S3.** Seasonal contributions of air temperature and other factors to winter soil temperature ( $T_{\text{soil}}$ ) variability at 40 cm and 160 cm depths during 1993–2011. (a,b) show the influence of autumn air temperature ( $T_{\text{air,Aut}}$ ), (c,d) show the influence of winter air temperature ( $T_{\text{air,Win}}$ ), and (e,f) show the contribution of other factors.

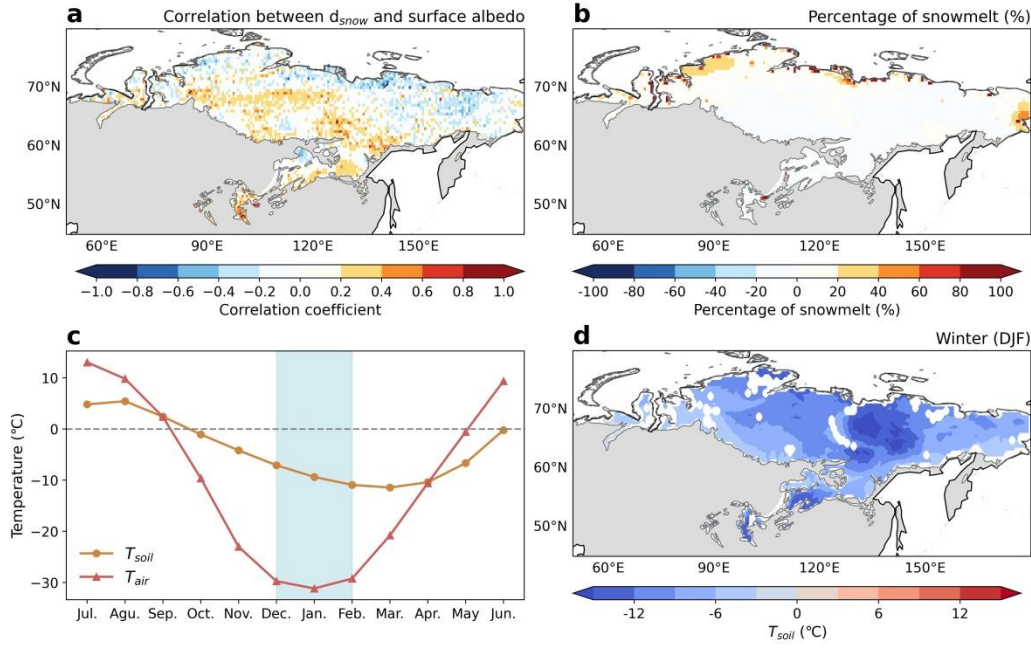


**Figure S4.** Relationship between snow thickness ( $d_{\text{snow}}$ ) and surface albedo, and snowmelt in winter over Siberia permafrost region. (a) Correlation between  $d_{\text{snow}}$  and surface albedo in winter during period 1993–2016. The areas with black hatching represent values significant at  $p < 0.05$  level by Student's t test. Surface albedo was obtained from the Global Land Surface Satellite (GLASS) broadband albedo product, offering an 8-day temporal resolution and a  $0.05^{\circ}$  spatial resolution, spanning period from 1981 to 2019. Monthly albedo values were obtained by averaging the 8-day composites. (b) Percentage of snowmelt to snow water equivalent (%) during the winter of 1993–2017, which reflects the impact of soil temperature on  $d_{\text{snow}}$ . (c) Annual variations in monthly air temperature ( $T_{\text{air}}$ ) and 40 cm soil temperature ( $T_{\text{soil}}$ ) averaged during 1993–2022. (d) Spatial distribution of mean (1993–2022) of winter  $T_{\text{soil}}$ .